STREAKING IMAGES THAT APPEAR ONLY IN THE PLANE OF DIFFRACTION IN UNDOPED GaAS SINGLE CRYSTALS: DIFFRACTION IMAGING (TOPOGRAPHY) BY MONOCHROMATIC SYNCHROTRON RADIATION

Masao Kuriyama, Bruce Steiner, Ronald C. Dobbyn, Uri Laor[1]

Institute for Materials Science and Engineering

National Bureau of Standards, Gaithersburg, Maryland 20899

and

David Larson and Margaret Brown

Grumman Aerospace Corporation

Bethpage, New York 11714-3580

PACS numbers: 61.10.Dp, 61.70., 68.35.p, 78.30F

Abstract

Streaking images restricted to the direction of the diffraction (scattering) vector have been observed on transmission through undoped GaAs. These disruption images (caused by the reduction of diffraction in the direction of observation) appear both in the forward and in Bragg diffracted directions in monochromatic synchrotron radiation diffraction imaging. This previously unobserved phenomenon can be explained in terms of planar defects (interfaces) or platelets which affects the absorption coefficient in anomalous transmission. Such regions of the crystal look perfect despite the presence of imperfections when the scattering vector is

not perpendicular to the normal of the platelets. The observed crystallographic orientation of these interfaces strongly indicates that they are antiphase boundaries.

I. Introduction

Streaking images, approximately (1~50 μm) X (200~300 μm), have been observed to appear only in the direction of $\underset{\sim}{H}$ in $(2\bar{2}0)$ and (400) transmission as disruptive images (reduction in x-ray intensity) in both the $\underset{\sim}{O}$ (forward) and $\underset{\sim}{H}$ (Bragg) diffracted beam directions at 8 and 10 Kev in synchrotron radiation monochromatic imaging. The direction of streaking rotates as the plane of diffraction defined by the incident beam and the scattering vector, $\underset{\sim}{H}$, is rotated. Figure 1a and b show enlarged $(2\bar{2}0)$ diffraction images of an undoped GaAs crystal in the $\underset{\sim}{O}$ and $\underset{\sim}{H}$ beam directions, respectively. Figure 2 shows an enlarged (400) image in the O beam direction of the portion of the crystal observed in Figure 1. In these images, the formation of "cellular structure"[2,3] is quite visible. With the monochromatic synchrotron radiation, the features of cellular structure are different in different diffraction conditions, in contrast to observation with Lang topography[4]. However, this cellular structure is not the subject of the present paper, and it will be discussed in a separate paper. This paper deals with the visibility of the streaking images. This phenomenon appears to be rather common in high resolution imaging in Laue (transmission) geometry and plays an important role in the identification of defect formation during crystal growth. A similar imaging mechanism was originally proposed in a brief appendix in a paper on magnetic domain walls[5]. This interruption mechanism in diffraction imaging now appears to

be more general. A detailed derivation of the effective absorption coefficient of planar defects (interfaces) and thin platelets randomly oriented will be given in this paper.

The sample crystal has a roughly square shape (8 mm X 8 mm) and is 0.8 mm thick. The surface normal is close to a cubic axis and is defined to be [001]. Diffraction images were observed with a video monitor for orientation and inspection of the overall quality of the crystal on the NBS materials science beam line, X23 A, at the National Synchrotron Light Source. The monochromatic beam was prepared [6-8] with a 2.5 cm X 3 cm cross section and less than 2 arc second divergence. The beam cross section was restricted by an x-y slit to the 1 cm^2 sample area in order to reduce background scattering. High resolution recording was made on nuclear emulsion plates.

II. Effective Absorption in Anomalous Transmission

For disruption images, the effective absorption coefficient, μ_{eff}, in both the 0 and H diffracted directions is given [9-13] by

$$\mu_{eff}^{(i)} = [1 + 2\,\gamma_H D_H^{(i)}(x)\,\exp(\Delta G(\underset{\sim}{H}))]\mu, \qquad (1)$$

where i is the mode of the dynamical field with i = 1 for anomalous transmission and $D^{(i)}_{\underset{\sim}{H}}(x)$ is the dynamical field strength of the i-mode with x indicating the deviation from the exact Bragg angle.

The quantity,

$$\gamma_H = F^i(\underset{\sim}{H})/F^i(\underset{\sim}{0}) \text{ with } F^i(\underset{\sim}{H}) = \sum_i \Delta f'' e^{-i\underset{\sim}{H}\cdot\underset{\sim}{r}_i}, \qquad (2)$$

is the ratio of the part of structure factor consisting of the imaginary part of atomic scattering factors for $\underset{\sim}{O}$ and $\underset{\sim}{H}$, which is close to one in most cases. The quantity μ is the ordinary linear absorption coefficient. Since $D^{(\frac{1}{g})}(x)$ is negative, μ_{eff} gives anomalous transmission. For simplicity and compactness, we show in Eq. (1) the expression for symmetrical diffraction. The following discussion applies equally to asymmetric diffraction.

The factor, $\Delta G(\underset{\sim}{K})$, describes crystal imperfection through the geometrical structure factor $g(\underset{\sim}{K})$:

$$\Delta G(\underset{\sim}{K}) = \frac{1}{2} \left(\Delta g(\underset{\sim}{K}) + \Delta g(-\underset{\sim}{K})\right), \qquad (3)$$

where $\underset{\sim}{K}$ is a momentum transfer and $\Delta g(\underset{\sim}{K})$ is the difference between the real structure factor, $g(\underset{\sim}{K})$, for an imperfect crystal and the structure factor, $g_p(\underset{\sim}{K})$, for the ideal perfect crystal. Thus,

$$\Delta g(\underset{\sim}{K}) = \frac{1}{NF(\underset{\sim}{K})} \left\{ \sum_{\underset{\sim}{\ell}} F_{\ell}(\underset{\sim}{K}) e^{-i\underset{\sim}{K}\cdot\underset{\sim}{u}(\underset{\sim}{\ell})} \; e^{-i\underset{\sim}{K}\cdot\underset{\sim}{\ell}} - \sum_{\underset{\sim}{\ell}} F(\underset{\sim}{K}) e^{-i\underset{\sim}{K}\cdot\underset{\sim}{\ell}} \right\}, \qquad (4)$$

where the lattice sum is restricted within the diffracting domain of atoms[11], F_{ℓ} is the x-ray (unit cell) structure factor of the ℓ-th cell, F is the x-ray structure factor of the unit cell in the perfect crystal, N is the number of unit cells in the diffracting domain of atoms, and $\underset{\sim}{u}(\underset{\sim}{\ell})$ is a displacement vector from the perfect lattice site, $\underset{\sim}{\ell}$. Since a real crystal does not have perfect periodicity, $\underset{\sim}{K}$ is given by $\underset{\sim}{H} + \underset{\sim}{q}$, where $\underset{\sim}{H}$ is a reciprocal lattice vector and $\underset{\sim}{q}$ is a vector indicating the deviation from the reciprocal lattice point.

The function $\Delta g(\underset{\sim}{K})$ can be rewritten

$$\Delta g(\underset{\sim}{K}) = \frac{1}{N} \sum_{\underset{\sim}{\ell}} \left(\frac{F_{\ell}(\underset{\sim}{K})}{F(\underset{\sim}{K})} e^{-i\underset{\sim}{K}\cdot\underset{\sim}{u}(\ell)} - 1\right) e^{-i\underset{\sim}{K}\cdot\underset{\sim}{\ell}}, \qquad (5)$$

where the lattice sum is taken within the diffracting domain of atoms. Unless this domain contains imperfections (i.e., $\underset{\sim}{u}(\underset{\sim}{\ell}) \neq \underset{\sim}{0}$), $\Delta g(\underset{\sim}{K})$ vanishes, resulting in the ideal anomalous transmission (see Eq. (1)).

As described in previous papers [9-13], the expression for the effective absorption coefficient, Eq(1), is valid for the anomalously transmitted beams both in the $\underset{\sim}{0}$ and $\underset{\sim}{H}$ beam directions in dynamical diffraction. The trajectory of these beams (the energy flow associated with photon fields inside the crystal) is identical to that expected in a perfect crystal. The propagation directions of the $\underset{\sim}{0}$ and $\underset{\sim}{H}$ beams outside the crystal are confined to the plane of diffraction. Beam divergence is suppressed during transmission. However, such divergence can be observed as contrast in images due to the scattering from imperfections located near the x-ray exit surface[11].

Let us define the beam geometry in Figure 3, where unit vectors, $\underset{\sim}{\sigma}$, $\underset{\sim}{t}$, and $\underset{\sim}{z}$ form an orthogonal set describing the normal to the plane of diffraction, the tangential direction of the incident beam and the thin crystal direction, respectively. The confinement of the diffracted beams within the plane of diffraction for these dynamical beams demands $\underset{\sim}{q}_{\sigma} = 0$. The diffraction vector, $\underset{\sim}{H}$, is in the plane of diffraction, and, $\underset{\sim}{h} = \underset{\sim}{H}/|\underset{\sim}{H}|$ defines the unit vector along $\underset{\sim}{H}$.

We postulate that the streaking images that we observe are due to platelet imperfections uniformly displaced by an amount $\underset{\sim}{u}_s$ with respect to the matrix at the interface. The orientation of a platelet is given by an orthogonal set of unit vectors, $\underset{\sim}{x}$, $\underset{\sim}{y}$ and $\underset{\sim}{n}$ as shown in Figure 3. The

vector, $\underset{\sim}{n}$, indicates the normal to the platelet face (the thin direction). The direction of $\underset{\sim}{y}$ is chosen to lie on the plane of diffraction. Figure 3 illustrates the situation where the diffracting domain of atoms (hatched) does not contain the platelet (imperfection).

In our model we further postulate homogeneous platelets, with a structure factor that is independent of ℓ within the platelet and given by $F'(\underset{\sim}{K}) = \langle F_\ell(\underset{\sim}{K})\rangle$, which may be different from $F(\underset{\sim}{K})$ for the matrix. The atomic displacement, $\underset{\sim}{u}(\underset{\sim}{\ell})$, in the surrounding matrix varies with ℓ to accommodate elastic compatibility. In addition, the diffracting domain of atoms is assumed to contain completely a given platelet.

Equation (5) can be resolved into platelet and matrix terms:

$$\Delta g(\underset{\sim}{K}) = \Delta g^{(1)}(\underset{\sim}{K}) + \Delta g^{(2)}(\underset{\sim}{K}), \tag{6}$$

where

$$\Delta g^{(1)}(\underset{\sim}{K}) = \frac{1}{N}\left[\frac{F'}{F}\exp(-i\underset{\sim}{K}\cdot\underset{\sim}{u}_s) - 1\right]\sum_{\ell} e^{-i\underset{\sim}{K}\cdot\underset{\sim}{\ell}}, \tag{7}$$

and

$$\Delta g^{(2)}(\underset{\sim}{K}) = \frac{1}{N}\sum_{\ell}\left[e^{-i\underset{\sim}{K}\cdot\underset{\sim}{u}(\underset{\sim}{\ell})} - 1\right] e^{-i\underset{\sim}{K}\cdot\underset{\sim}{\ell}}. \tag{8}$$

The bracketed quantity in the latter term is normally approximated by $-i\underset{\sim}{K}\cdot\underset{\sim}{u}(\underset{\sim}{\ell})$, which is observed as Huang scattering.[14,15] Huang scattering depends on odd power terms of $\underset{\sim}{K}$, resulting in $\Delta g^{(2)}(\underset{\sim}{H}) + \Delta g^{(2)}(-\underset{\sim}{H}) = 0$. Thus Huang scattering does not influence anomalous transmission. Even terms in $\Delta g^{(2)}(\underset{\sim}{K})$ can be handled as change in the Debye-Waller factor for Eq(1). This long range strain effect in the matrix through $\Delta g^{(2)}(\underset{\sim}{K})$

results only in scattering images[11], which, as we have noted, are suppressed in the body of the crystal.

The main task is now to obtain the lattice sum in Eq.(7) in the diffracting domain of atoms. The summation over $\underset{\sim}{\ell}$ of $\exp[-i\underset{\sim}{K}\cdot\underset{\sim}{\ell}]$ can be replaced by that of $\exp[-i\underset{\sim}{q}\cdot\underset{\sim}{\ell}]$ for all diffraction vectors. It is convenient to introduce another orthogonal coordinate system $O\text{-}\rho h\sigma$, where the units vectors $\underset{\sim}{\rho}$,$\underset{\sim}{h}$ and $\underset{\sim}{\sigma}$ represent the directions of the classical energy flow, the diffraction vector, $\underset{\sim}{H}$, and the normal to the plane of diffraction, respectively. Figure 4 illustrates the projection of the volume common to both a platelet and the diffracting domain onto the plane of diffraction. The origin of the coordinate system is set at the center of this volume.

We consider this platelet, whose thickness is D (Figure 5). The cross section of the platelet in a plane perpendicular to the plane of diffraction is shown in Figure 5, where the y axis is perpendicular to the plane of the figure, the x' direction is the projection of the x axis (or the $\underset{\sim}{n}$ axis) on the plane of diffraction, and the $\underset{\sim}{\sigma}$ is the normal to the plane. The size, $D/\sin\chi$, of the platelet in the x' direction remains constant, regardless of the position of the plane of diffraction (in the $\underset{\sim}{\sigma}$-direction), except for the edge portions of the platelet. χ is the angle between $\underset{\sim}{\sigma}$ and $\underset{\sim}{n}$. The size limits the range of the lattice sum in the $\underset{\sim}{\rho}$ direction to $2W = D/\sin\chi\,\sin\phi$, as shown in Figure 4. The angle ϕ is the angle between $\underset{\sim}{h}$ and the projection of the platelet normal, n, onto the plane of diffraction, that is $\underset{\sim}{n}_\perp$:

$$\cos\phi = (\underset{\sim}{h}\cdot\underset{\sim}{n}_\perp), \tag{9}$$

where

$$\underset{\sim}{n}_{\perp} = \frac{\underset{\sim}{n} - (\underset{\sim}{n}\cdot\underset{\sim}{q})\underset{\sim}{q}}{|\underset{\sim}{n} - (\underset{\sim}{n}\cdot\underset{\sim}{\sigma})\underset{\sim}{\sigma}|} \quad . \tag{10}$$

The lattice sum is now given by

$$\sum_{\underset{\sim}{\ell}} e^{i\underset{\sim}{q}\cdot\underset{\sim}{\ell}} = \sum_{\sigma} e^{-iq_\sigma \ell_\sigma} \cdot \sum_{h} e^{-iq_h \ell_h} \cdot \sum_{\rho} e^{-iq_\rho \ell_\rho} \quad ,$$

where the σ-summation is limited to the width of the platelet, the h-summation to the range determined by the coherent beam size in the h direction, say, -a to + a, and the ρ- summation to the range - W + $\ell_h \cot\phi$ to W + $\ell_h \cot\phi$. As mentioned before, the anomalously transmitted beam is restricted to the plane of diffraction, so that $\underset{\sim}{q}_\sigma$ = 0. The σ-summation becomes the projected width of the platelet. Thus,

$$\frac{1}{N}\sum_{\underset{\sim}{\ell}} e^{-\underset{\sim}{q}\cdot\underset{\sim}{\ell}} = \frac{1}{N}\sum_{\sigma}\sum_{h} e^{-iq_h \ell_h} \sum_{\rho} e^{-iq_\rho \ell_\rho}$$

$$\rightarrow \left(\frac{1}{V}\right) W_\sigma \int_{-a}^{+a} dh\, e^{-iq_h h} \int_{-W+h\cot\phi}^{W+h\cot\phi} d\rho\, e^{-iq_\rho \rho}$$

$$= \left(\frac{1}{V}\right) W_\sigma \int_{-a}^{+a} dh\, e^{-i(q_h + q_\rho \cot\phi)h} \int_{-W}^{+W} d\rho'\, e^{-iq_\rho \rho'} \quad , \tag{11}$$

where the lattice sum $(1/N)\sum$ is replaced by $(1/V)\int d\sigma dh d\rho$.

Performing the integration, we obtain

$$\frac{1}{N}\sum e^{-i\underset{\sim}{q}\cdot\underset{\sim}{\ell}} = \frac{V_p}{V}\,\frac{\sin[(q_h+q_\rho\cot\phi)a]}{(q_h+q_\rho\cot\phi)a}\,\frac{\sin(q_\rho W)}{q_\rho W}\quad , \tag{12}$$

where (Vp/V) is the volume ratio of the platelet within the diffracting domain of atoms. For a very thin platelet ($W\to 0$), the spherical Bessel function of zero order of $q_\rho W$ is one, regardless of the value of q_ρ. No restrictions are imposed on the momentum transfer in the ρ direction; the reciprocal lattice points are elongated in the direction of thickness. The condition for anomalous transmission guarantees that $q_h = 0$ for the $i = 1$ mode in the thick crystal case. Since q_ρ can take any value, the spherical Bessel function of $[q_\rho\cot\phi]a$ is effectively zero, unless $\cot\phi = 0$. When $\cot\phi = 0$, this function becomes one. In other words, only when the diffraction vector, $\underset{\sim}{H}$, is perpendicular to the projection of the platelet normal onto the plane of diffraction, does the function, $\Delta G(\underset{\sim}{K})$, not vanish:

$$\Delta G(\underset{\sim}{K}) = \frac{V_p}{V}\left[\frac{F'}{F}\cos\underset{\sim}{K}\cdot\underset{\sim}{u}_s - 1\right] \quad . \tag{13}$$

Thus, when $\cot\phi = 0$, and thus $\cos\phi = 0$, the effective absorption coefficient is given by

$$\mu_{eff}^{(1)} = \left[1 + 2\gamma_H D_H^{(1)}(x)\,\exp\left[\frac{V_p}{V}\left(\frac{F'}{F}\cos\underset{\sim}{H}\cdot\underset{\sim}{u}_s - 1\right)\right]\right]. \tag{14}$$

From Eq. (9), the condition on ϕ states that

$$(\underset{\sim}{H}\cdot\underset{\sim}{n}_i) = 0, \tag{15}$$

which is equivalent from Eq. (10) to

$$(\underset{\sim}{H}\cdot\underset{\sim}{n}) = 0, \tag{16}$$

because $(\underset{\sim}{H}\cdot\underset{\sim}{\sigma}) = 0$. When $\cot\phi \neq o$ and thus $\Delta G(\underset{\sim}{K})=0$,, the crystal looks perfect despite the presence of such platelet imperfections. Images of those platelets that satisfy condition (16) appear to be streaked because the longest dimension of the platelets lies only in the direction of H. Such images are the projection of the imperfections onto a plane parallel to the x-ray exit surface.

III. Discussion

When we have a distribution of thin platelets, those platelets whose surface normal is perpendicular to the diffraction vector, H, are visible through their disruption of diffraction. Others with a different orientation do not disrupt anomalous transmission and are thus invisible in the given diffraction. As given by Eq. (14), the effective absorption coefficient is dependent also upon the $\underset{\sim}{H}\cdot\underset{\sim}{u}_s$ term as well as upon the atomic constituents, F', which may differ from those in the matrix. Normally in diffraction imaging (topography), the condition for invisibility is simply given through the $\underset{\sim}{H}\cdot\underset{\sim}{u}$ relationship. Features can vary in visibility for various $\underset{\sim}{H}$'s with a cosine dependence. In contrast to this situation, the thin extended planar defects modeled here have a unique visibility condition, given by Eq. (16), in addition to normal visibility conditions, such as the $\underset{\sim}{H}\cdot\underset{\sim}{u}$ relationship and the dependence on the imperfection volume ratio. The explicit expression for the effective absorption coefficient

given here for symmetrical diffraction also gives the correct effective volume change in $\Delta G(\underset{\sim}{H})$ for asymmetric diffraction.

In $(2\bar{2}0)$ and (400) images of undoped GaAs, those thin platelets with [110] orientation are imaged in the $\underset{\sim}{0}$ and $\underset{\sim}{H}$ beams for $(2\bar{2}0)$ diffraction, while those with [011] and $[0\bar{1}1]$ orientation are imaged in the (400) diffraction. The $(2\bar{2}0)$ images indicates that the thickness of the platelets is of the order of 1μm (resolution limit). The projected width of these platelets in the (400) images is roughly 60 μm. In both cases, their length is 200 ~ 300 μm.

Experiments with asymmetric diffraction condition will confirm the F' and $\underset{\sim}{u}_s$ dependence. Comparison of etch-pits patterns with these streaking images is also desirable.

Several different structures are consistent with the observation made thus far. The essential conditions are that coherence is preserved between platelets and matrix and that there be a phase shift at the platelet/matrix interface. The platelets may simply be low angle grain boundaries, or they may represent regions of subtle changes in stoichiometry, impurities, or drastic changes such as precipitates or voids. The interfacial strain may include stacking faults. However, the fact that the observed interfaces are {110} planes strongly favors antiphase boundaries as a likely structure, where Ga and As atoms change places along a <111> direction parallel to the interface. The formation of such antiphase boundaries creates the interfacial displacement, $\underset{\sim}{u}_s$. Indeed, the {110} planes associated with these observations are distinguished from {100} and {111} planes in that both types of atoms are contained in the former. Understanding of these platelets will shed light on the formation of cellular

structure in undoped GaAs. These "streaking" images have been observed in In doped GaAs as well accompanied by individual dislocations (presumably decorated) images.

Acknowledgements

The authors acknowledge the support of the U. S. Department of Commerce and of the National Aeronautics and Space Administration, through the Center for the Development of Crystal Growth in Space. The NBS Materials Science synchrotron radiation beam line is located at the National Synchrotron Light Source, Brookhaven National Laboratory, which is supported by the U. S. Department of Energy, Division of Materials Science (DOE contract number DE-AC02-76-CH00016).

REFERENCES:

1. Permanent address: Crystals Department, Nuclear Research Centre-Negev, P. O. Box 9001, Beer-Sheva, 84190, Israel.
2. S. Clark, and D. J. Stirland, Microscopy of Semiconducting Materials (Institute of Physics, London) pp. 339-344 (1981).
3. T. Kitano, J. Matsui, and T. Ishikawa, Jpn J. Appl. Phys. 24 L948 (1985).
4. E. Zielinska-Rohozlnska, J. Cryst. Growth 87 154-156 (1988).
5. E. J., Boettinger, H. E. Burdette, and M. Kuriyama, Phil. Mag. 36 763-776 (1977).
6. R. Spal, R. C. Dobbyn, H. E. Burdette, G. G. Long, W. J. Boettinger, and M. Kuriyama, Nuclear Instr. and Methods 222 189-192 (1984).
7. M. Kuriyama, R. C. Dobbyn, S. Takagi, and L. C. Chow, Medical Physics 14 (6) Nov/Dec 968-974 (1987).

8. M. Kuriyama, in Advanced Techniques for Microstructure Characterization ed. T. R. Anatharaman and R. Krishnan (1988) Trans. Tech. Publ. Aedermannsdorf, Switzerland.

9. M. Kuriyama, Phys. Stat. Sol. 24 743-748 (1967).

10. M. Kuriyama, W. J. Boettinger, and H. E. Burdette, Advances in X-Ray Analysis, ed. H. F. McMurdie, C. S. Barrett, J. B. Newkirk, and C. O. Ruud, (New York, Plenum) Vol. 20 p. 245-257 (1977).

11. M. Kuriyama, W. J. Boettinger, and G. G. Cohen, Ann. Rev. Sci. 12 23-50 (1982).

12. W. J. Boettinger, H. E. Burdette, E. N. Farabaugh, and Kuriyama, M., Advances in X-Ray Analysis ed. H. F. McMurdie, C. S. Barrett, J. B. Newkirk, and C. O. Ruud, (Plenum, New York), Vol. 20, p. 207-219, (1977).

13. M. Kuriyama, and J. G. Early, Acta Cryst. A 30 525-535 (1974).

14. Krivoglaz, M. A.: Theory of X-Ray and Thermal Neutron Scattering by Real Crystals, Plenum, New York (1969).

15. P. H. Dederichs, J. Phys. F 3 471-496 (1973).

FIGURE CAPTIONS:

Fig. 1. Images of diffracted beams in $(2\bar{2}0)$ transmission from undoped gallium arsenide with monochromatic 8 Kev synchrotron radiation.
a: 0-diffracted beam, and
b: H diffracted beam.
Cellular structure is also visible along with streaking images running in the $[1\bar{1}0]$ direction.

Fig. 2. Image of the 0-diffracted beam in (400) transmission of the portion of the crystal in Figure 1. This image was taken with monochromatic 10 Kev synchrotron radiation. The streaking images run in the [100] direction.

Fig. 3. The beam geometry with respect to the crystal and a platelet. $\underset{\sim}{q}$: the normal to the plane of diffraction, $\underset{\sim}{t}$: the direction of the incident beam projected on the crystal surface, and $\underset{\sim}{z}$: the thin crystal direction. The diffraction vector, $\underset{\sim}{H}$, is given by $\underset{\sim}{k}_H - \underset{\sim}{k}_0$ and is in the plane of diffraction. The orientation of a platelet is given by an orthogonal set $\underset{\sim}{x}$, $\underset{\sim}{y}$ and $\underset{\sim}{n}$. $\underset{\sim}{n}$: normal to the platelet face. $\underset{\sim}{y}$ is chosen to lie on the plane of diffraction. This figure illustrates the situation where the diffracting domain of atoms (hatched) does not contain the platelet.

Fig. 4. The projection of the volume (hatched) common to both a platelet and the diffracting domain onto the plane of diffraction. x' is the direction of the projection of the $\underset{\sim}{x}$ axis (and the $\underset{\sim}{n}$ axis) on the plane of diffraction. The units vector $\underset{\sim}{\rho}$, $\underset{\sim}{h}$ and $\underset{\sim}{q}$ represent the directions of the classical energy flow, the diffraction vector $\underset{\sim}{H}$ and the normal to the plane of diffraction, respectively. $\underset{\sim}{n}_1$ is the projection of the platelet normal on the plane of diffraction, $\underset{\sim}{q}$ is perpendicular to the plane of this figure, ϕ is the angle between h amd n_1. 2W is the thickness of the platelet in the $\underset{\sim}{\rho}$ direction.

Fig. 5 The cross section of the platelet in a plane perpendicular to the plane of diffraction. The y axis is perpendicular to the plane of the figure. D is the thickness of the platelet. χ is the angle between $\underset{\sim}{q}$ and $\underset{\sim}{n}$. The hatched region indicates the limit of the lattice sum at a given position of the plane of diffraction along the $\underset{\sim}{q}$ direction.

Fig 1a

Fig 1b

Fig 2

Fig. 3

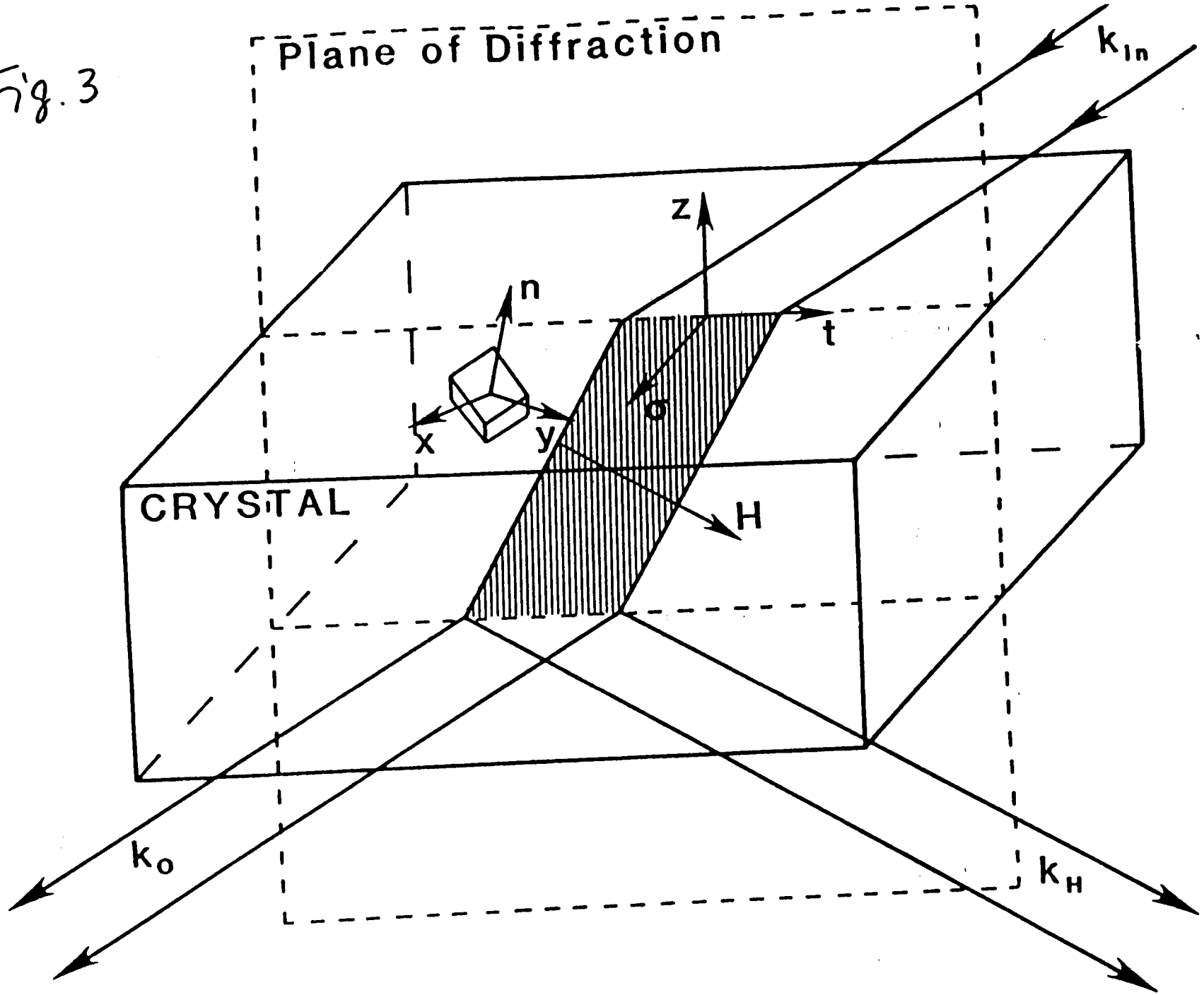

Fig. 4

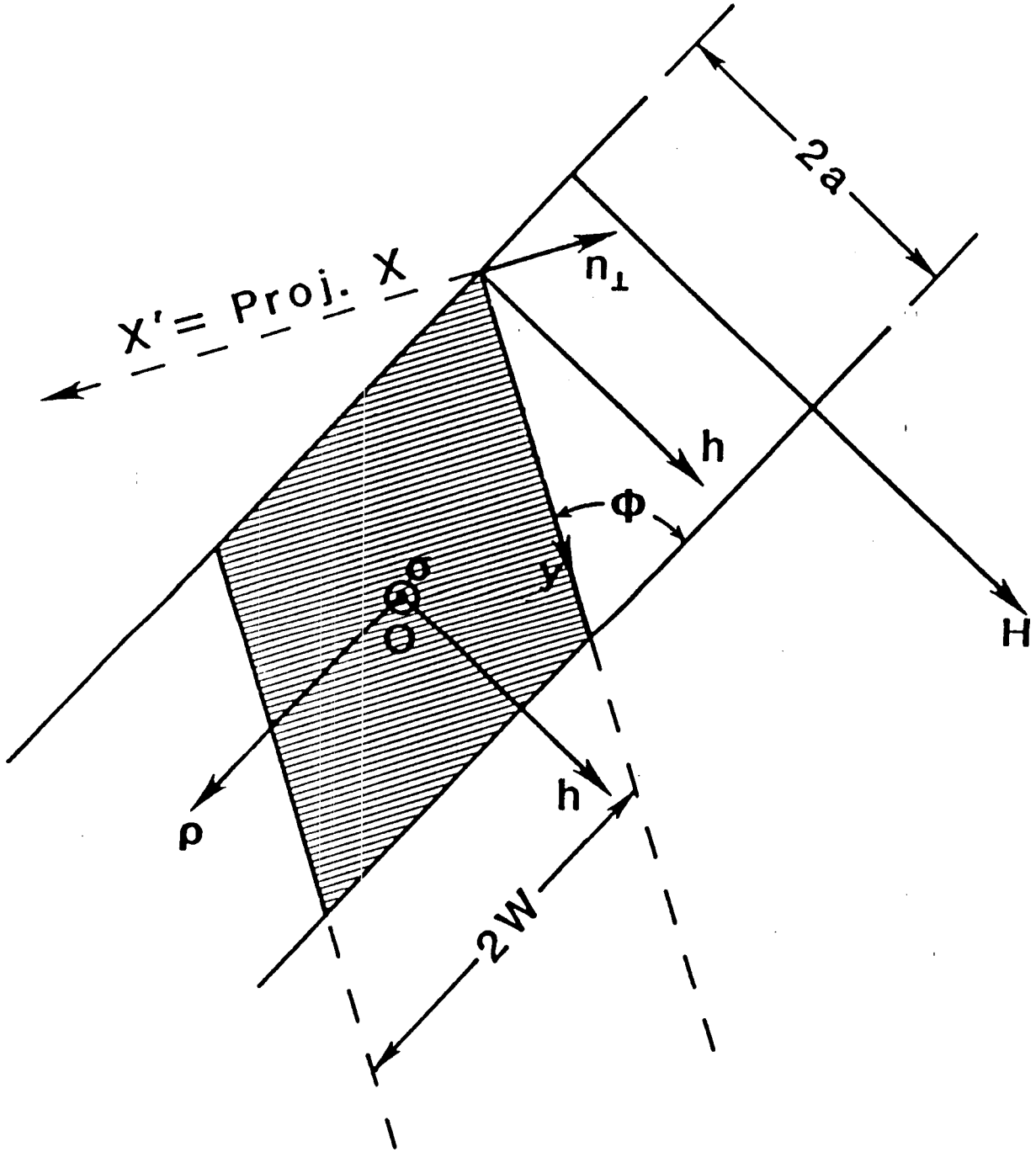

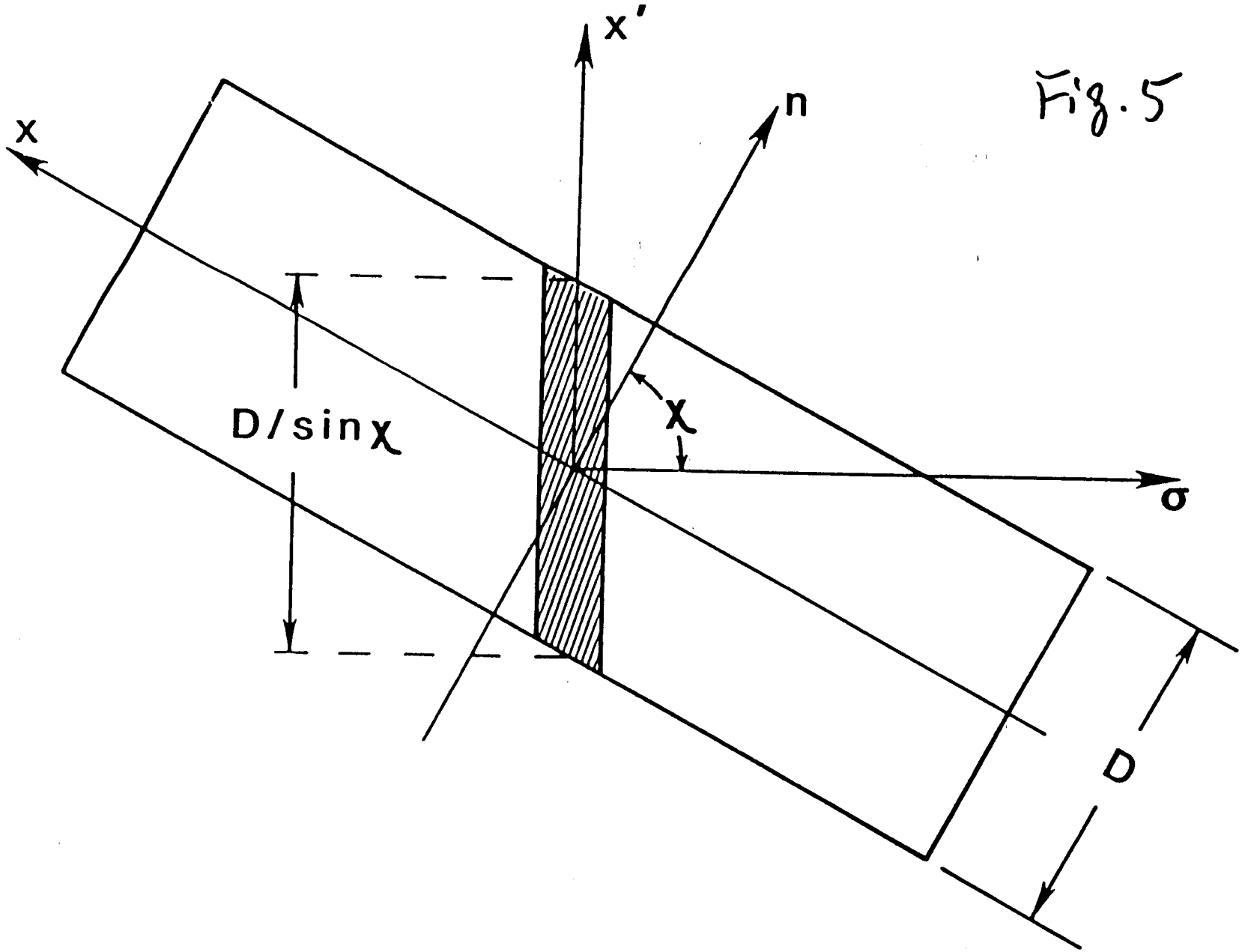

Fig. 5